JOURNAL OF SOLID STATE CHEMISTRY **13**, 288–297 (1975)

The Compounds and the Phase Diagram of MoO_3-Rich Bi_2O_3–MoO_3 System

TU CHEN

Xerox Palo Alto Research Center, Palo Alto, California 94304

AND

G. S. SMITH

Chemistry Department, Lawrence Livermore Laboratory, Livermore, California

Received May 23, 1974

The equilibrium phase diagram between 0 and slightly above 50 mole % Bi_2O_3 in the Bi_2O_3–MoO_3 system has been studied by differential thermogravimetric analysis (DTA) and X-ray diffraction measurements on fused mixtures and single crystals. The results confirm the existence of the four compounds α ($Bi_2O_3 \cdot 3MoO_3$), β ($Bi_2O_3 \cdot 2MoO_3$), γ ($Bi_2O_3 \cdot MoO)_3$ and ε ($\sim 1.3Bi_2O_3 \cdot MoO_3$) in the system. However, the phase diagram as well as the nature of melting of the α and γ were found disagreed with previous results. The γ compound melts incongruently at 947°C, whereas the α compound melts congruently at 662°C. The crystal class and lattice parameters of the compounds were determined based on the single crystal as well as powder pattern techniques. The results show that all four compounds have the monoclinic structure. The unit cell parameter of the β, γ, and ε compounds were found to be quite different from previously reported data. The lattice parameters obtained from X-ray analysis were also verified by density measurements of the single crystals. The polymorphism of the compounds was also investigated with single crystal samples. No polymorphic transformations for the α, β, and γ phases were detected in the work.

Introduction

The phase diagram and compounds of the Bi_2O_3–MoO_3 system have been the subject of several studies. Belyaev and Smolyaninov (*1*) and Bleijenberg et al. (*2*) both reported two congruently melting compounds, $Bi_2O_3 \cdot 3MoO_3$ (α) and $Bi_2O_3 \cdot MoO_3$ (γ), in the region 0–50 mole% Bi_2O_3. Studies by Erman and co-workers on the phase diagram (*3*) and structures of the compounds (*4–7*) gave rather different results. These investigators found a third compound, $Bi_2O_3 \cdot 2MoO_3$ (β), in this composition range and another phase (ε) having solid solubility with a composition of $\sim$1.4 $Bi_2O_3 \cdot MoO_3$. They reported moreover, that the α, β, and γ compounds are formed by peritectic reactions and that the β and γ compounds each have several crystallographic modifications.

We present here additional studies of the Bi_2O_3–MoO_3 system from 0 to just past 50 mole % Bi_2O_3 by DTA and X-ray diffraction methods. We were able also to grow large single crystals of the α, β, and γ phases, and our work includes studies of these materials.

Experimental

Polycrystalline specimens of the required mole fraction were prepared by fusion of 99.99% pure MoO_3 and 99.999% pure Bi_2O_3 powders purchased from Atomergic Chemical Co. After thorough blending, the powders were melted in a covered Pt crucible, and the melts were then cast into a water-cooled Pt dish. Casted specimens were ground to –200 mesh powders. About 2 g of each specimen were sent to Metallurgical Laboratory Inc. for wet chemical analysis.

TABLE I

CHEMICAL ANALYSIS OF THE SINGLE CRYSTALS

	Nominal Composition		Compositions determined by the analyses				
	mole%		wt%		mole%		
Compound	Bi_2O_3	MoO_3	Bi_2O_3	MoO_3	Bi_2O_3	MoO_3	Remarks
$Bi_2O_3 \cdot 3MoO_3$ (α)	25.0	75.0	51.9	48.1	25.0	75.0	Grown from 20 mole% Bi_2O_3 solution
$Bi_2O_3 \cdot 2MoO_3$ (β)	33.33	66.67	61.81	38.37	33.23	66.77	Grown from 27.5 mole% Bi_2O_3 solution
$Bi_2O_3 \cdot MoO_3$ (γ)	50.0	50.0	76.21	23.53	50’01	49.99	Grown from 45 mole% Bi_2O_3 solution
$\sim 13Bi_2O_3 \cdot 10MoO_3$ (ε)	56.5	43.5	80.11	19.58	55.83	44.17	Grown from 50 mole% Bi_2O_3 solution

Large single crystals of the α, β, γ and phases were grown by pulling with a seed from molten solutions. Several solutions in the range of 20–25 mole% Bi_2O_3 provided crystals of α; crystals of β, γ, and ε were grown from 27.5, 45, and 50 mole% Bi_2O_3, respectively. Chemical analyses for these single crystals are listed in Table I.

Crystals of α and γ phases were also grown by slow cooling of Bi_2O_3–MoO_3 molten solution consisting of 20 mole% Bi_2O_3 and 40 mole% Bi_2O_3, respectively, at a cooling rate of 2°/min. These crystals proved to be the same as the α and γ crystals obtained by the above method.

The DTA measurements were made on pulverized samples and on single crystal specimens with a DuPont 900 DTA instrument. Prior to these measurements (and X-ray powder pattern measurements), the polycrystalline samples were annealed overnight at temperatures of 600–670°C. For our thermograms we typically used about 15 mg of samples placed in a Pt-lined microcrucible. The rates of heating and cooling were 5°/min. These thermograms often showed irreproducible exothermic peaks in the cooling cycle. The appearance of these extraneous peaks seems to be related to the migration of molten material during thermal cycling. The use of high-purity Al_2O_3 microcrucibles eliminated the extraneous peaks. Temperatures used for the construction of the phase diagram were those observed on the heating cycle taken with the Pt-lined crucible. The temperature of the liquidus point of some of the mixtures was taken from the cooling curve. In this case, the correction of the temperature due to the supercooling was made with the same amount of supercooling obtained from other transformations in the thermogram.

Powder X-ray diffraction patterns were recorded on a GE XRD-5 diffractometer under high X-ray intensity generated at 40 kV and 32 mA. High resolution was obtained by using a 1° beam slit and 0.05° detector slit. Weissenberg and precession cameras were used in diffraction studies of single crystals to obtain preliminary lattice constants as well as space group extinctions. We used the program of Evans et al. (*8*) to refine the lattice constants. The X-ray wavelength standards are, for Cu radiation: $K\alpha_1 = 1.54051$ Å and $K\alpha_2 = 1.54433$ Å.

Densities of single crystal specimens were measured by Archimedes method.

Results and Discussion

1. Single Crystals

Figure 1 shows large crystals of the α (a), β (b) and γ (c) compounds pulled from 20,

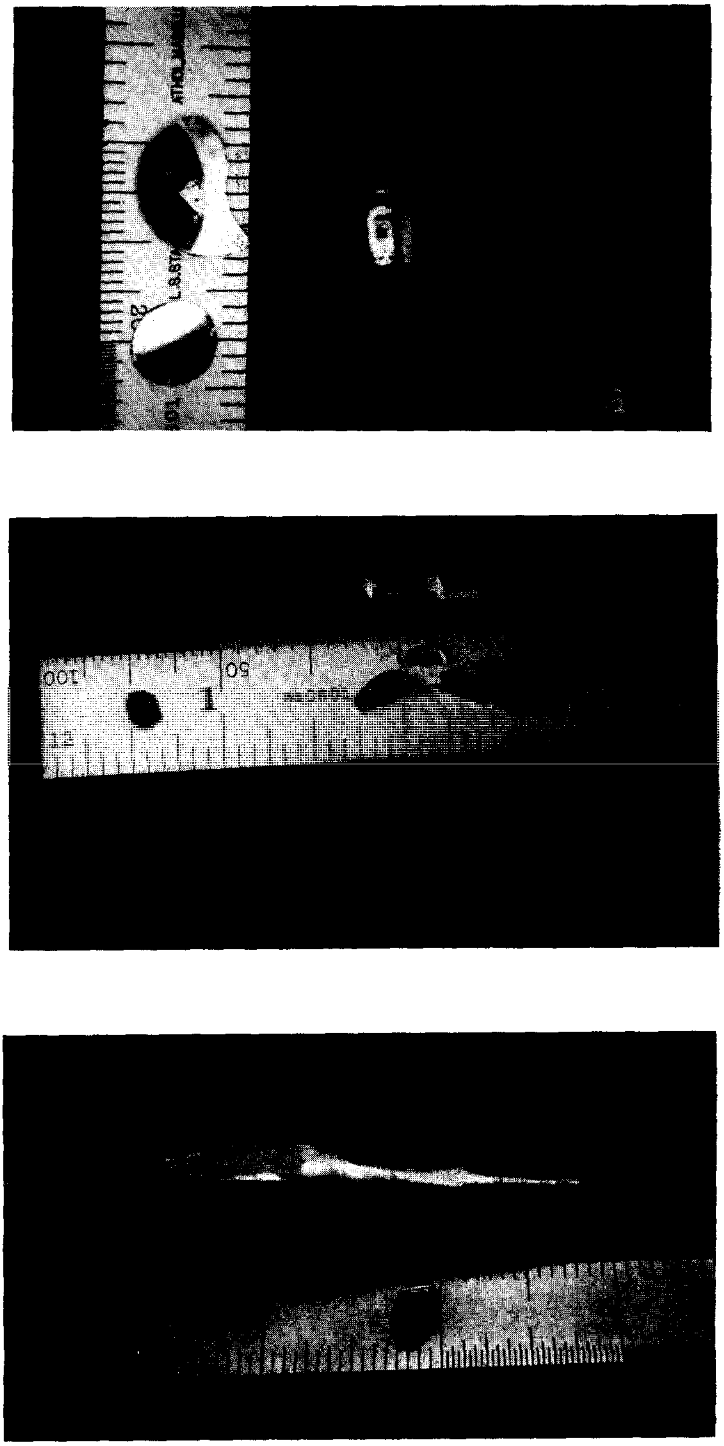

FIG. 1. Single crystal of α (a), β (b), and γ (c) phases.

27.5, and 45 mole% Bi_2O_3 molten solutions, respectively. The colors are uniform throughout each crystal and are: greenish-yellow for α, brownish-yellow for β, and light yellow for γ.

As shown in Table I, these crystals have a stoichiometric composition of Bi_2O_3:MoO_3 of 1:3, 1:2 and 1:1, respectively, for the α, β, and γ phases, although they were grown from off-stoichiometric compositions. Evidence, particularly from X-ray diffraction studies, indicates that the α, β, and γ phases are line compounds (or virtually so).

Crystal boules pulled from molten solutions of 1:1 molar composition show a Bi_2O_3:MoO_3 ratio of ~1.26. Diffraction patterns for these crystals are different from those of the γ phase. The color of the boule is light yellow at its crust and deep yellow toward the center. Also, the density measured on a piece from the crust is different from that of a piece near the center. We believe this modification corresponds to the ε phase of Erman et al. (*3*) and that the phase does indeed have solid solubility.

2. *Equilibrium Phase Diagram*

Figure 2 shows the phase diagram for the composition range studied. Apart from DTA runs on crystals of the ε phase, the region between γ and ε was not investigated in detail. Therefore, dotted lines based on the phase diagram published by Erman et al. (*3*) are indicated in this range.

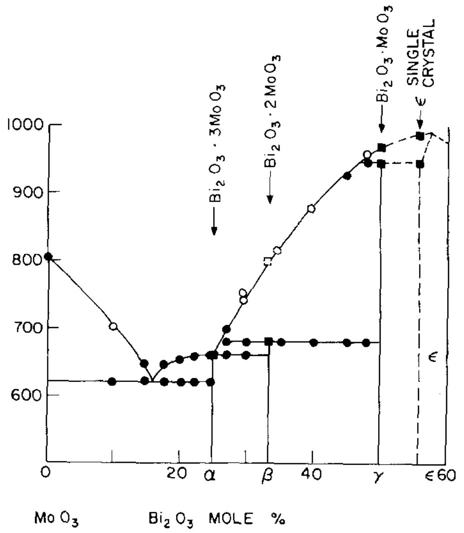

FIG. 2. Partial equilibrium phase diagram of the Bi_2O_3–MoO_3 system, ● from polycrystalline sample—heating; ○ from polycrystalline sample—cooling; ■, from single crystals—heating; □ from single crystals—cooling.

In many respects the phase diagram is similar to the one given by Erman et al. (*3*) We find a eutectic between MoO_3 and α; a peritectic reaction at 682°C between liquid and γ to form β; a peritectic reaction at 947°C between liquid and ε to form γ. The corresponding temperatures from the diagram of Erman et al. (*3*) are somewhat lower: 650 and 920°C, respectively.

We, however, do find two major points of disagreement: (1) In the region between α and about 20 mole% Bi_2O_3 only two phase boundaries are encountered; accordingly, the α phase is a congruently melting compound (mp = 662°C) or a limiting case of a eutectic or peritectic reaction. (2) No solid state transformation of γ just below 900°C was detected.

These conclusions are supported by DTA runs and high-temperature X-ray diffraction studies of γ phase.

In Figure 3 a single endothermic peak, corresponding to melting, appears in the heating curve of the α compound. The absence of an additional endothermic peak in the subsequent remelting indicates congruent melting. Furthermore, powder patterns taken following melting of such a sample shows only the α compound.

The heating curve of a γ crystal shows (Fig. 3) a strong endothermic peak at 947°C and small endothermic inflection at 973°C. The former corresponds to the noncongruent melting point and the latter to the liquidus. No other thermal effects were observed in the heating; none in particular were seen just below 900°C. Moreover, in high-temperature X-ray diffraction studies taken at 825 ± 5°C and 925 ± 5°C, no new lines appear which would indicate a phase transformation.

We have previously mentioned the appearance of spurious peaks in the DTA cooling curves when Pt microcrucibles were used to contain the samples. (Indeed, several of these are seen in the cooling curves of Fig. 3.) However, we did not see extra peaks when A_2O_3 microcrucibles were used. Failure to

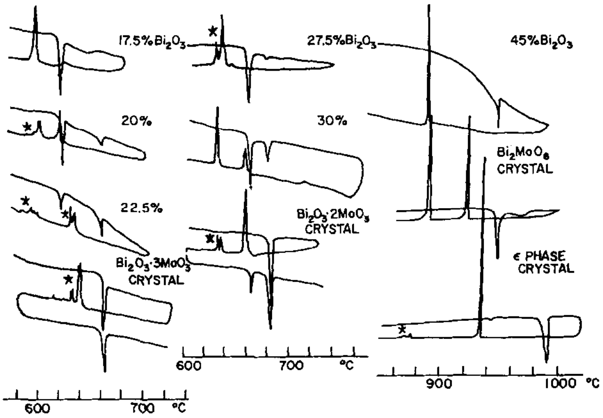

FIG. 3. DTA traces; peaks marked with * are the spurious peaks.

TABLE II

X-RAY POWDER DIFFRACTION DATA FOR β (Bi$_2$O$_3$·2MoO$_3$)

d_{obsd} (Å)	d_{calcd} (Å)	$h\,k\,l$	I_{obsd}	d_{obsd} (Å)	d_{calcd} (Å)	$h\,k\,l$	I_{obsd}
8.014	7.993	0 1 1	7	2.274	2.279	1 1 5	1
6.652	6.644	1 1 1	13	2.274	2.273	2 4 2	1
5.949	5.942	0 0 2	12	2.196	2.197	3 4 1	3
5.215	5.206	0 1 2	8	2.174	2.175	0 2 5	5
4.919	4.917	0 2 1	3	2.174	2.172	5 1 2	5
4.780	4.786	2 1 1	13	2.145	2.144	4 3 2	3
4.212	4.213	2 0 2	3	2.048	2.051	5 2 2	2
3.924	3.925	2 1 2	3	2.048	2.046	5 0 3	2
3.795	3.797	2 2 1	3	1.992	1.992	6 0 0	8
3.781	3.777	3 0 1	4	1.980	1.981	0 0 6	8
3.448	3.446	0 3 1	2	1.947	1.947	3 4 3	33
3.308	3.311	1 3 1	3	1.846	1.846	6 2 1	2
3.209	3.206	3 2 0	95	1.757	1.759	4 2 5	1
3.197	3.194	0 2 3	100	1.751	1.750	3 1 6	1
3.164	3.164	3 1 2	5	1.691	1.690	6 2 3	7
3.081	3.079	0 3 2	2	1.686	1.685	3 2 6	13
2.989	2.987	4 0 0	5	1.640	1.640	3 6 0	13
2.974	2.971	0 0 4	2	1.640	1.639	0 6 3	13
2.823	2.821	3 2 2	2	1.632	1.631	5 4 3	10
2.809	2.809	3 0 3	32	1.632	1.628	3 4 5	10
2.787	2.786	1 1 4	2	1.604	1.603	6 4 0	10
2.700	2.700	0 4 0	17	1.596	1.596	0 4 6	10
2.591	2.591	4 1 2	1	1.403	1.404	6 0 6	4
2.554	2.553	4 2 1	1	1.289	1.289	9 2 0	8
2.459	2.458	0 4 2	3	1.282	1.282	0 2 9	2
2.435	2.436	3 3 2	4	1.266	1.266	6 6 3	13
2.409	2.410	2 4 1	2	1.266	1.263	3 6 6	13
2.409	2.408	1 4 2	2	1.216	1.216	3 8 3	5
2.393	2.393	4 2 2	2	1.140	1.141	9 4 3	4
2.328	2.321	0 1 5	1				

TABLE III

X-RAY POWDER DIFFRACTION DATA FOR $\gamma(Vi_2O_3 \cdot MoO_3)$

h k l	d_{obsd}	d_{calcd}	I_{obsd}	*h k l*	d_{obsd}	d_{calcd}	O_{obsd}
1 0 0	17.293	17.251	7	7 1 0	2.449	2.459	4
1 1 0	13.703	13.673	15	7 2 0	2.409	2.407	2
0 2 0	11.262	11.211	17	0.10.0	2.241	2.242	4
1 2 0	9.408	9.400	9	1.10.0	2.223	2.224	2
2 0 0	8.638	8.625	4	5 7 1	2.168	2.168	4
1 3 0	6.868	6.858	2	8 0 0	2.158	2.156	5
2 3 0	5.655	5.648	18	8 3 0	2.072	2.072	4
3 3 0	4.557	4.558	4	6 8 0	2.007	2.007	49
1 5 0	4.341	4.340	1	0 8 2	1.977	1.977	9
4 1 0	4.240	4.235	1	9 4 1	1.729	1.729	12
2 3 1	3.978	3.981	2	$\bar{9}$ 4 1	1.721	1.721	12
0 6 0	3.738	3.737	2	3.12.1	1.694	1.694	18
4 3 0				$\bar{3}$.12.1	1.692	1.692	24
3 4 1	3.268	3.268	51	6 8 2	1.634	1.634	5
$\bar{3}$ 4 1	3.249	3.249	60	$\bar{6}$ 8 2	1.625	1.625	4
5 3 0	3.133	3.132	2	5.13.1	1.486	1.488	2
0 6 1	3.103	3.105	1	$\bar{5}$.13.1		1.485	
2 6 1	2.922	2.926	2	12.0.0	1.438	1.438	3
$\bar{2}$ 6 1		2.917		0.16.0	1.401	1.401	4
6 0 0	2.875	2.875	100	0 0 4	1.397	1.395	2
0 8 0	2.802	2.803	39	9.12.1	1.302	1.303	4
4 6 1	2.527	2.526	1	$\bar{9}$.12.1	1.299	1.299	4
7 0 0	2.465	2.464	4	6.16.0	1.260	1.260	7

reckon with artifacts of this kind could of course result in a serious misinterpretation of the DTA data. It is possible that the claim of Erman et al. (*3*) for the noncongruent melting of α, and more than two phase boundaries for mixtures between α and ~20 mole % Bi_2O_3 is related to such artifacts.

Finally, the results of our X-ray diffraction studies from powder patterns of polycrystalline and single crystal specimen confirm the phase boundaries shown in Fig. 2. That is to say, all powder patterns in this composition region are composites of the basic patterns of MoO_3, α, β, and γ. Moreover it is found that in the various mixtures the diffraction lines corresponding to α, β, and γ do not shift by measurable amounts. Therefore, we believe these compounds do not have solid solubility.

3. *X-Ray Diffraction Studies*

Powder patterns obtained from single crystals of the compounds show excellent agreement with the pattern published for the α phase (*9*), but considerable difference with patterns reported (*4*, *6*, *9*, *12*) for β and γ phases. Tables II and III give, respectively, diffraction data of the β and γ phases obtained in this work. Diffraction data was obtained also for the ε phase. Except for some low intensity diffraction lines, our *d*-spacing data agree reasonably well with those reported recently by Miyazawa et al. (*13*) for the compound "3 $Bi_2O_3 \cdot 2$ MoO_3."

Our diffraction studies of single crystal specimens show that the compounds in general have relatively large unit cells and are often characterized by pseudosymmetry and subcells.

In the following the crystal data of each compound obtained in this work (Table IV) and those of previous investigations (Table V) will be compared and discussed.

(*a*) α *Compound* ($Bi_2O_3 \cdot 3MoO_3$). The crystal data obtained for this compound are in

TABLE IV

CRYSTAL DATA OF PRESENT RESULTS[a]

Compound	Molar ratio $Bi_2O_3:MoO_3$	Unit cell constant (Å) *a*	*b*	*c*	*β*	Cell volume (Å^3)	Space group	Density (g/cm$_3$) Calcd	Expt	Number of molecular per unit cell	Remarks
α	1:3	7.715 (0.0009)[a]	11.512 (0.0012)	11.981 (0.0013)	115°26.0′ (0.6′)	960.99 (0.13)	$P2_1/c$	6.204	6.22	4	Similar to Ref. (*9*) and (*10*)
β	1:2	11.954 (0.001)	10.810 (0.001)	11.890 (0.001)	90°[c]	1536.5 (0.2)	$P2_1/n$	6.517	6.545	8	Similar to β phase of Ref. (*7*)
γ	1:1	17.251 (0.001)	22.422 (0.002)	5.851 (0.002)	89°.30.2′ (0.6′)	2158.60 (0.6)	$P2_1/c$	7.506	7.495	16	
ε	1:0.79±	24.723 (0.003)	5.804 (0.001)	11.799 (0.003)	102°45.48′ (0.9)	1651.7 (0.4)	$P2_1/m$ or $P2_1$	7.536[b]	7.47–7.53		Nonstoichiometric compound

[a] Value of standard error.

[b] Calculated based on 13 Bi_2O_3 + 10 MoO_3 molecular per unit cell.

[c] β deviates from 90° by less than 0.1°.

excellent agreement with the results of Aykan (*9*) and Ce Sari et al. (*10*). On the other hand, in work on the α compound formed by coprecipitation from salt solution, van den Elzen and Rieck (*14*) reported significantly smaller lattice constants and measured density, and gave the Bi:Mo ratio for their material as 2:2.85. Thus nonequilibrium stoichiometries are indicated for the α phase prepared by coprecipitation. Unit cell parameters and density obtained by Erman et al. (*7*) differ from the other reported data, and the discrepancy cannot be expalined.

(*b*) *β Compound* (*$Bi_2O_3 \cdot 2MoO_3$*). Except for a slight difference in the unit cell parameters and the measured density, the crystal data of this compound obtained in this work are in agreement with data of the β phase (obtained from annealed coprecipitated powder or sintered oxide) reported by Erman et al. (*7*). The β′ form which was formed by coprecipitation of the salt solution as reported by Erman et al. (*7*) was not investigated in this work. We have investigated the possibility of polymorphism by studying single crystal specimens quenched from annealing temperatures up to the melting point of the compound. However, the metastable β″ form of the β phase observed by Erman et al. (*7*) in a specimen quenched from the fused oxides was not observed in this work.

Crystals of the β phase are pseudo orthorhombic, and a subcell is clearly evidenced in the diffraction photographs. The diffraction symmetry not only approaches that of *mmm*, but there is also an additional systematic extinction beyond those required by $P2_1/n$, namely *hk0* missing for *k* odd. No splitting between *hkl* and $\bar{h}kl$ spectra were observed in the powder patterns. Accordingly, the monoclinic angle, β, is given as 90°. Any deviation from 90° is estimated as less than 0.1°. That the true symmetry is monoclinic is confirmed by the observation of a conspicuous *dispersed extinction* when crystals of the β phase are viewed along [010] direction under a polarizing microscope (*11*).

The crystal structure is based on a subcell with edges: $a/3 \times b/2 \times c/3$. This is a pseudo body-centered tetragonal cell of dimensions, 4.0 × 5.4 × 4.0 Å. In consequence of the

TABLE V

CRYSTAL DATA OF PREVIOUS WORKS

Compound	Phases reported and method of preparation	Molar ratio $Bi_2O_3.MoO_3$	Unit cell constant (Å)				Cell volume (Å)^3	Space group	Density		References
			a	*b*	*c*	*β*			Calcd.	Expt.	
α	α—Single crystal from fused oxides	1:3	7.85	11.70	12.25	116°20′	1010	$P2_1/c$	5.99	5.86	Erman et al. (*7*)
	α—Coprecipitated from salt solutions		7.719	11.516	11.985	115°25′			6.197	6.14	Ayken (*9*)
	α—Coprecipitated		7.719	11.502	11.982	115°29′		$P2_1/c$			Cesari et al (*10*)
	α—Coprecipitated and fused		7.685	11.491	11.929	115°24′		$P2_1/c$		5.97	Van den Elzen (*14*)
β	β—Annealed powder from coppt. or sintering	1:2	11.86	10.79	11.89	90°±10′	1520	*Pn*	6.64	6.38	Erman et al. (*7*)
	β″—Quenched phase from fused oxide		11.97	10.79	11.89		1540	*Cmca*	6.55		Erman et al. (*7*)
γ	γ—Natural Koechlinite	1:1	5.49	16.19	5.49						Powder File (JCPDS)
	γ—Synthetic Koechlinite coppt. from salt solution		5.502	16.213	5.483				8.28	8.26	Ayken et al. (*7*)
	γ—Synthetic Koechlinite from salt solution		5.500	16.215	5.485		490		8.25	8.00	Erman et al. (*7*)
	γ—Sintered oxides at 750°C		3.95		17.21						Blasse (*12*)
	γ′—Sintered or fused oxides or annealed coppt. above 550°C		11.90	11.90	5.45		770		7.85	7.80	Erman et al. (*7*)
	γ″—Sintered or fused oxides or annealed coppt. below 550°C		17.22	22.40	5.60	89°30′	2160		7.45	7.30	Erman et al. (*7*)

subcell, diffraction maxima are strong for *h* and l = 3*n* and *k* = even.

(*c*) *γ Compound* (*$Bi_2O_3 \cdot MoO_3$*). In agreement with other studies involving fused oxides (*7*, *9*, *12*), the crystal data we obtained for this compound are quite different from natural or synthetic Koechlinite. The data which show the greatest similarity to our results are the lattice parameters of the γ'' phase reported by Erman et al. (*7*). However, the nonstoichiometric molar ratio of Bi_2O_3: MoO_3 = 1–1.2:1 obtained by them and the metastability of the phase are in disagreement with the present results.

Crystals of the γ phase are also pseudo-orthorhombic. However, with fine-resolution optics on our diffractometer, splitting between *hkl* and $\bar{h}kl$ spectra here clearly observed. The monoclinic symmetry was also confirmed by the observation of a *dispersed extinction* for crystals viewed along [010] direction under a polarizing microscope.

The crystal structure of γ is based on a subcell having edges: *a*/3, *b*/4, and *c*. This is a pseudo face-centered cubic cell approximately 5.6 Å on a side. The subcell previously mentioned for the β compound is a variant of this pseudo face-centered cubic subcell.

Our γ-phase unit cell accounts for the powder lines (only ten in number) given by Blasse (*12*). His tetragonal unit cell is related to ours as follows: $c_{\text{Tet}} = a_\gamma$; $a_{\text{Tet}} = \sqrt{2}/2\ c_\gamma$; $b_{\text{Tet}} = \sqrt{2}/2\ b/_{\gamma}4$.

Erman et al. (*7*) have suggested that γ is the low-temperature and Koechlinite the high-temperature form. Our high-temperature diffraction and DTA studies give no indications of any polymorphism. Moreover, Koechlinite is considerably more dense (~10%) than the γ form. Hence it is not reasonable that Koechlinite should be the high-temperature phase. Rather, it seems that Koechlinite is the low-temperature stable form, the higher density value reflecting larger coordination numbers for the cations as compared with our γ phase. Transformations, necessarily then of a reconstructive type, of γ to Koechlinite could be expected to be sluggish. In this connection, we note that Koechlinite readily forms from aqueous solutions at mild temperatures (*9*).

(*d*) *ε Compound*. Crystals of this phase belong to the monoclinic system. The lattice parameters listed in Table V are for crystals with a molar ratio of Bi_2O_3:MoO_3 = 1.26:1. For other compositions within the solid solution range of this compound, slightly different values of the lattice constants could result.

The crystal data reported recently by Miyazawa et al. (*13*) for a phase they term 3 $Bi_2O_3 \cdot 2MoO_3$ are in reasonable agreement with our results for the ε compounds. These authors give a value for *c* which is twice our value, but list no lines with *l* odd in their powder pattern data. Furthermore, it is misleading to call this phase a 3:2 compound. Their published chemical analysis corresponds actually to Bi_2O_3:MoO_3 = 1.30:1. Further work on this compound is needed to determine the extent of the solid solubility.

An interesting correlation between densities and composition of the compounds was obtained from the results of this work. As shown in Fig. 4 the plot of density versus composition of the compounds including that of pure MoO_3 show that the density of the compounds increases almost linearly from pure MoO_3 to the γ compound. This correlation might be accidental; however, it may indicate the existence of a structural similarity between the compounds.

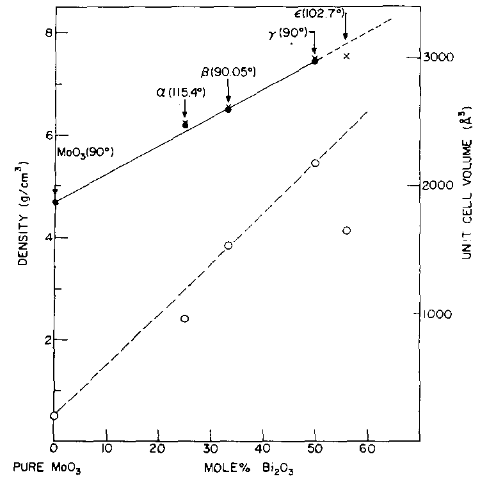

FIG. 4. Density and cell volume dependence of the compounds as function of Bi_2O_3 concentration. ● Calcd. density; × expt density; ○ calcd. cell volume.

Conclusion

The equilibrium phase diagram of the MoO_3 rich Bi_2O_3–MoO_3 system based on the fused oxides has been presented. The results show some differences from the existing phase diagrams.

The existence of the α ($Bi_2O_3 \cdot 3MoO_3$), β ($Bi_2O_3 \cdot 2MoO_3$), and γ ($Bi_2O_3 \cdot MoO_3$) phases in the phase diagram was confirmed by DTA and X-ray analyses on non-stoichiometric mixtures as well as single crystals of the compounds. The existence of $\varepsilon \cdot (\sim 13\ Bi_2O_3 : 10\ MoO_3)$ phase in the binary system as reported by Erman et al. (*3*) was also confirmed by growth and analyses of the single crystals of the compound.

Based on DTA and crystal growth of single crystals, it was determined that the β and γ phases are formed by peritectic reactions and the α compound exists as a limiting case of a peritectic or eutectic reaction.

The crystal class and lattice parameters of the compounds were also determined in this work. The results show that except for the α phase, there are many differences that exist between our results and the existing data.

The polymorphism of the compounds prepared from fused oxides were also investigated. In contrast with some of the previous investigations, our studies detected no polymorphic transformations for the α, β, and γ phases.

Acknowledgment

We would like to thank B. Charlan for his assistance in sample preparation and single crystal growth.

References

1. I. N. Belyaev and N. P. Smolynaninov, *Russ. J. Inorg. Chem.* (Engl. Transl.) **7**, 579 (1962).
2. A. C. A. M. Bleizenberg, B. C. Lippens, and G. C. A. Shuit, *J. Catal.* **4**, 581 (1958).
3. L. Ya. Erman, E. L. Calperin, and B. P. Soboler, *Russ. J. Inorg. Chem.* (Engl. Transl.) **16**, 258 (1971).
4. L. Ya. Erman, E. L. Galpérin, I. K. Kolchin, G. F. Dobrazakanskii, and K. S. Chernshev, *Russ. J. Inorg. Chem.* (Engl. Transl.) **9**, 1174 (1964).
5. L. Ya. Erman and E. L. Galpérin, *Russ. J. Inorg. Chem.* (Engl. Transl.) **11**, 122 (1966).
6. L. Ya. Erman and E. L. Galpérin, *Russ. J. Inorg. Chem.* (Engl. Transl.) **13**, 487 (1968).
7. L. Ya. Erman and E. L. Galpérin, *Russ. J. Inorg. Chem.* (Engl. Transl.) **15**, 441 (1970).
8. H. T. Evans, Jr., D. E. Appelman, and D. S. Handwerker, "Unit Cell Refinement Program", U.S. Geological Survey, Washington, D.C.
9. K. Aykan. *J. Catal.* **12**, 281 (1968).
10. M. Cesari, G. Perego, A. Zazzetta, G. Manara, and B. Natori, *J. Inorg. Nucl. Chem.* **33**, 3595 (1971).
11. T. Chen, *J. Crystal Growth* **20**, 29 (1973).
12. G. Blasse, *J. Inorg. Nucl. Chem.* **28**, 1124 (1966).
13. S. Miyazawa, A. Kawana, H. Loizumi, and H. Iwasaki, *Mat. Res. Bull.* **9**, 41 (1974).
14. A. F. van den Elzen and G. D. Rieck, *Acta Cryst.* **B29**, 2433 (1973).